The Inter-Flare Variability of Lyman-alpha Emission in Equivalent Magnitude Solar Flares

Harry J. Greatorex[1], Ryan O. Milligan[1], Phillip C. Chamberlin[2]

1. *Astrophysics Research Centre, School of Mathematics & Physics, Queen's University Belfast, University Road, Belfast, BT7 1NN, UK*
2. *Laboratory for Atmospheric and Space Physics, University of Colorado Boulder, Boulder, CO, USA*

Science and Technology Facilities Council

Abstract

The chromospheric Lyman-alpha line of neutral hydrogen (Lyα; 1216 Å) is the most intense emission line in the solar spectrum and is believed to constitute a considerable portion of the total radiated energy in solar flares. Here, we present a multi-wavelength study of three M3 flares that were simultaneously observed by RHESSI, GOES, and SDO. Despite having identical X-ray magnitudes these flares show significantly different Lyα responses. The peak Lyα enhancements above quiescent background for these flares were 1.5 %, 3.3 %, and 6.4 %. However, the predicted Lyα enhancements from FISM2 were consistently <2.5 %. Examining the properties of the nonthermal electrons derived from spectral analysis of HXR observations, an association was found between δ and the peak irradiance enhancements in Lyα. Finally, the percentage of nonthermal energy radiated in the Lyα line during the impulsive phase was found to range from 2–8 %. Comparatively, the radiative losses in He II (304 Å) were found to range from 0.6-1.4 %. These results may have significant implications for space weather studies and atmospheric modelling, as well as influence the interpretation of flare-related Lyα observations in Solar Cycle 25.

Observations & Analysis

For this study, a sample of three M3 flares were examined. Figure 1 shows the SDO/AIA images for each flare in 94 Å and 304 Å. Figure 2 details the co-observations for each flare from RHESSI, GOES, and SDO.

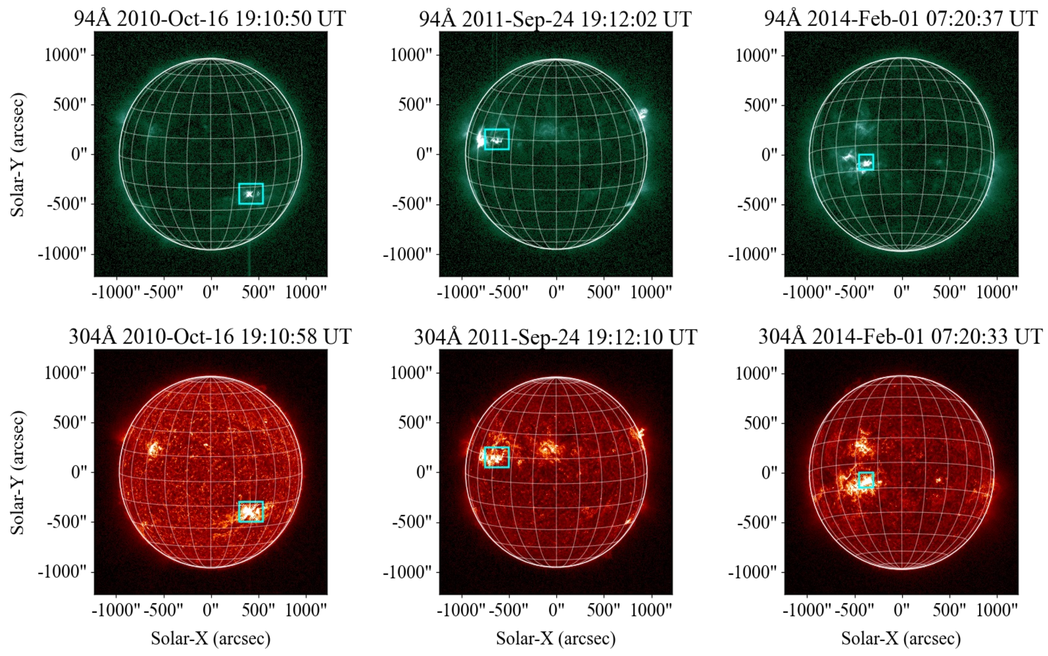

Figure 1: *Images taken from SDO/AIA for each flare in the* 94 Å *(top row) and* 304 Å *(bottom row) filters approximately centered around their HXR peaks. Each column represents a single flare and the timestamp of each image is shown in the title above each frame. Cyan annotations in each image indicate the flaring region.*

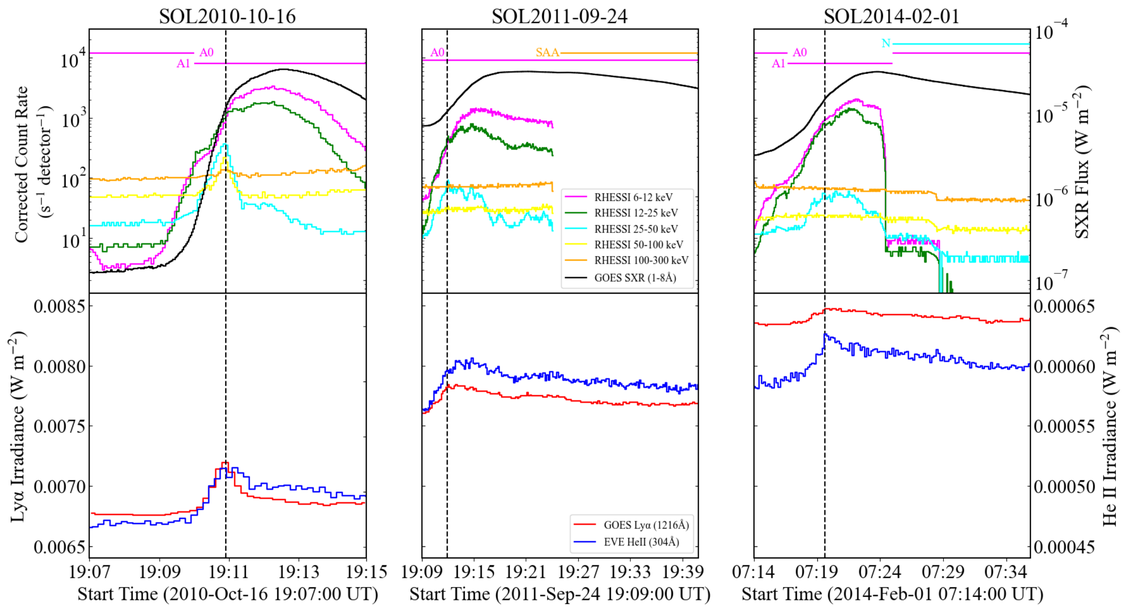

Figure 2: *Top Row: HXR lightcurves from RHESSI in discrete energy bands. The data also includes flags indicating attenuator state changes, SAA crossings, and RHESSI night (horizontal lines). SXR lightcurves from GOES/XRS in the 1–8 Å wavelength range (black solid). Bottom Row: Observed Lyα (red) and He II (blue) irradiance from GOES/EUVS-E and SDO/EVE, respectively. The vertical dashed line in each panel represents the peak of the 25–50 keV band for each flare.*

For each flare, normalised Lyα and He II lightcurves were compared to estimated irradiance profiles from FISM2. From this, the peak enhancement in each component could be determined to observe the variability in emission between flares. Following this, the HXR spectra from RHESSI were analyzed for each flare to determine the variability in nonthermal electron parameters. Specifically, a thick target model was fit to the nonthermal portion of the HXR spectrum in 12s intervals across the impulsive phase of each flare, returning the spectral index (δ), low energy cut-off (Ec), and electron rate (A) for each interval (Figure 3). These could then be applied in Equation 1 to calculate the energy deposited into the chromosphere by nonthermal electrons. Finally, the contribution of Lyα and He II to the radiated energy budget was determined by converting from irradiance observed at Earth to power radiated at the Sun, integrating over the impulsive phase, and comparing to the total nonthermal energy.

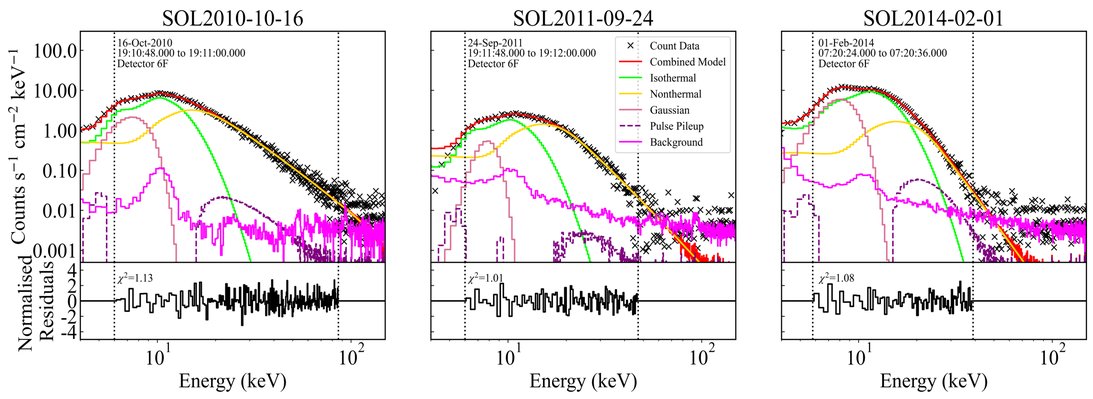

Figure 3: *RHESSI count spectra for detector 5 at the HXR peak in each flare. Overlaid are the individual and combined fit components. The dotted line indicated the upper and lower energy limits. The bottom panels show the residuals in each energy bin.*

Results

Part A | Irradiance Variability

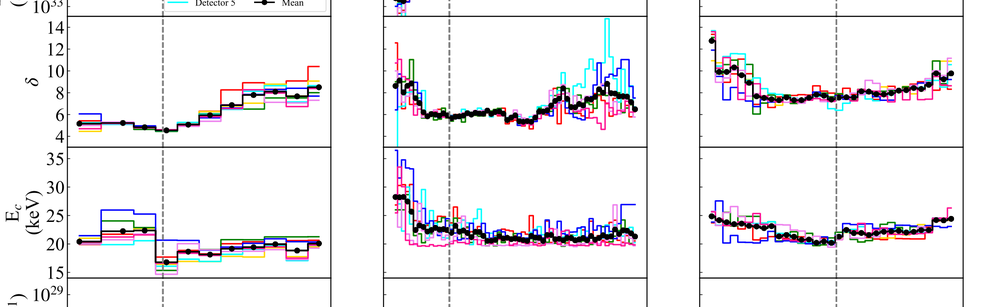

Figure 4: *Normalised irradiance profiles for each of the three flares. Red and blue curves correspond to Lyα and He II data, respectively. Solid lines correspond to observational data from GOES/EUVS-E and SDO/EVE while dashed lines correspond to the predicted irradiance profiles from FISM2.*

Flare	Peak Lyα Enhancement		Peak He II Enhancement	
	GOES/EUVS-E	FISM2	SDO/EVE	FISM2
SOL2010-10-16	6.4%	2.2%	10.8%	10.7%
SOL2011-09-24	3.1%	0.7%	7.3%	0.4%
SOL2014-02-01	1.5%	0.9%	7.4%	3.3%

Table 1: *Peak irradiance enhancements in Lyα and He II for each flare.*

Part B | HXR Spectroscopy

Figure 5*: Temporal evolution of the nonthermal parameters for each flare as derived from RHESSI HXR spectroscopy. First row: electron rate (A). Second row: spectral index (δ). Third row: low energy cutoff (Ec). Fourth row: nonthermal electron power (Pnth). Fifth row: reduced χ2 value for the combined fit model at each interval. The vertical dashed grey line indicates the peak time of the RHESSI 25–50 keV energy band.*

Flare	A	δ	Ec	Pnth
	(10^{35} electrons s^{-1})		(keV)	(10^{28}erg s^{-1})
SOL2010-10-16	4.2 ± 1.3	4.6 ± 0.1	16.8 ± 1.8	1.5 ± 0.4
SOL2011-09-24	1.1 ± 0.3	5.7 ± 0.2	21.8 ± 1.3	0.5 ± 0.1
SOL2014-02-01	2.7 ± 1.2	7.4 ± 0.4	20.2 ± 0.5	1.0 ± 0.4

Table 2: *Values of nonthermal fit parameters at the peak of the 25–50 keV HXR emission and the associated peak nonthermal electron power.*

Part C | Flare Energetics

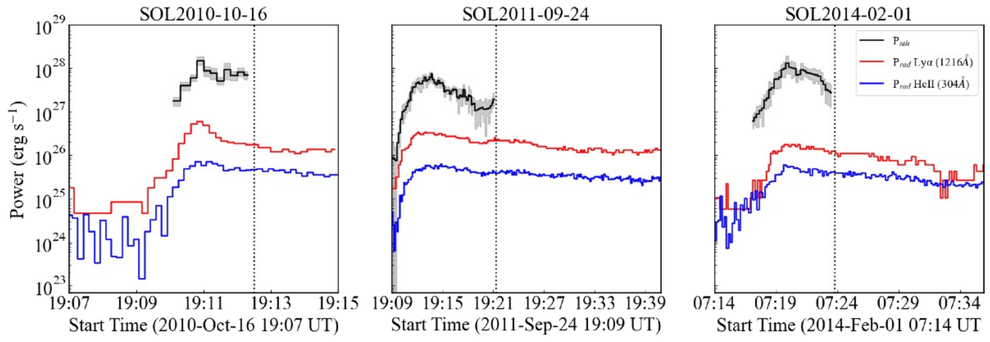

Figure 6*: Nonthermal and radiated power as a function of time for each flare in the sample. The dashed lines indicate the impulsive phase integration limits. The black shaded region in represents Pnth ± σ, where σ is taken as the as the standard deviation of Pnth over each RHESSI detector.*

Flare	Time Range (UT)	Total Energy (erg)			Erad/Enth (%)	
		Nonthermal Electrons	Lyα	He II	Lyα	He II
SOL2010-10-16	19:09:00 – 19:12:30	$9.7 \pm 1.6 \times 10^{29}$	1.3×10^{28}	7.1×10^{27}	4.4 ± 0.7	0.7 ± 0.1
SOL2011-09-24	19:07:00 – 19:21:20	$2.0 \pm 0.3 \times 10^{30}$	1.6×10^{29}	2.9×10^{28}	7.9 ± 1.1	1.4 ± 0.2
SOL2014-02-01	07:14:00 – 07:23:47	$2.3 \pm 0.7 \times 10^{30}$	1.7×10^{28}	1.5×10^{28}	2.0 ± 0.6	0.6 ± 0.2

Table 3: Total energy in nonthermal electrons and radiated components during each flare.

Conclusions

- Irradiance enhancements in Lyα and He II found to vary from 1.5-6.4% across equivalent magnitude flares.
- FISM2 significantly underpredicts Lyα and He II flux enhancements during solar flares.
- Relationship found between spectral index and enhancement in Lyα emission.
- Lyα and He II may radiate up to a combined total of 9.3% of the flare energy during the impulsive phase.

References & Acknowledgements

H.J.G would like to thank the UK's Science & Technology Facilities Council (ST/W507751/1) for supporting this research. R.O.M would like to thank the UK's Science & Technologies Facilities Council for the award of an Ernest Rutherford Fellowship (ST/N004981/2). H.J.G and R.O.M. would both like to thanks Prof. Mihalis Mathioudakis for several stimulating discussions and initial feedback on this work. H.J.G would like to further thank the UK's Science & Technologies Facilities Council for the award of Long Term Attatchment funding to fascilitate an extended visit to NASA Goddard Space Flight Centre to conduct research in collaboration with Dr. Graham Kerr. H.J.G would also like to thank Dr. Brian Dennis for his valuable guidance and advice on the techniques used as part of this research.